

# An Introduction to Pure Shift NMR

Authors: Paul Bowyer, NMR Applications Specialist, JEOL U.K. (Ltd.), and Ronald Crouch, NMR Applications Consultant, JEOL USA, Inc.

## What is Pure Shift NMR?

The proton is the most frequently studied nucleus in NMR because of its chemical abundance and high sensitivity.  $^1\text{H}$  spectra are rich in chemical information, but their narrow chemical shift range and extensive overlap of multiplet structure complicate spectral analysis and interpretation. ‘Pure shift’ NMR spectroscopy (also known as broadband homonuclear decoupling) has been developed for unravelling these overlapped proton NMR spectra. Resulting spectra are considerably simplified as they consist of single lines, reminiscent of proton-decoupled  $^{13}\text{C}$  spectra at natural abundance, with no multiplet structure, as shown in Fig. 1.

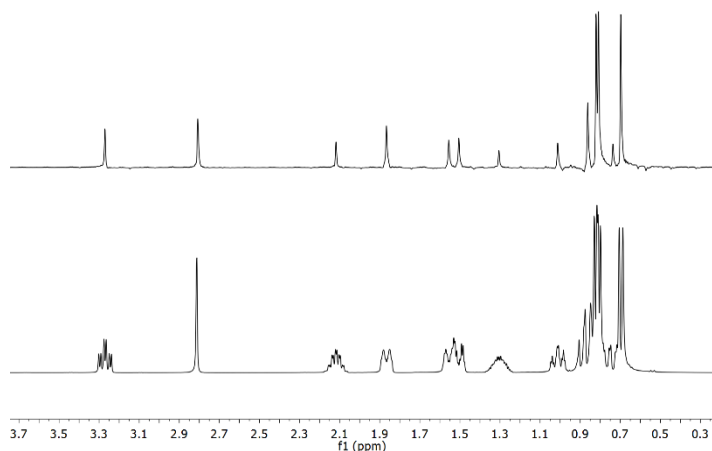


Figure 1. 400 MHz  $^1\text{H}$  (bottom) and pure shift (top) spectra of menthol. Multiplet peaks in the  $^1\text{H}$  spectrum appear as singlets in the pure shift spectrum.

Pure shift has proven particularly useful for the highly overlapped proton spectra found, for example, in reaction mixtures, natural products and biomacromolecules. More recently, pure shift has also been applied to new fields such as metabolomics studies.

In this whitepaper, a short history of the development of pure shift NMR and an introduction to the most widely used pure shift experiments are given, including important experimental parameters and other practical considerations.

## Experimental

All the spectra presented in this paper were collected on standard 400 MHz or 500 MHz JEOL ECZ spectrometers equipped with 5 mm ROYAL HFX probes using Delta 5.3.1 software. The pulse programs used were optimized for performance and are available upon request.

## A Brief History of Pure Shift

The history of pure shift NMR is almost as old as NMR spectroscopy itself. As early as 1963, Ernst described the theoretical use of stochastic high-frequency fields that could “remove all spin-spin couplings at the same time”[1]. However, it was not until 1976 that full broadband homonuclear spectra were first published, again by Ernst and coworkers[2]. In their work, they showed how a  $45^\circ$  projection of a homonuclear 2D J-resolved spectrum could yield a broadband homonuclear decoupled  $^1\text{H}$  spectrum. Unfortunately, due to the magnitude-mode required for 2D J-resolved spectra, lines in the pure shift spectrum obtained by this method are usually broad.

In 1982, Pines and coworkers showed the acquisition of pure shift spectra using a bilinear rotational decoupling (BIRD) experiment[3]. At the time, the method they described required the pulse sequence to be repeated for each point of the pure shift FID, making it very slow to acquire a high-resolution spectrum, but nevertheless it laid the foundations for many of the pure shift developments that were to follow.

However, it was not until 1997, when Zangger and Sterk published their paper on pure shift using slice-selective acquisition[4], that pure shift took the necessary leap forward from being an esoteric method with limited applicability, to being a powerful technique for improving spectral resolution across a wide range of samples and applications. At around the same time, Krishnamurthy introduced the band-selective homonuclear decoupled (BASHD)[5] approach as a way of removing homonuclear splittings in the indirect dimension of homonuclear 2D spectra.

The heightened interest in pure shift, largely driven by Zangger and Sterk’s seminal paper, meant that method development continued apace and another significant leap forward was made in 2014 with the advent of the PSYCHE experiment[6], which brought about significant gains in sensitivity, robustness and ease-of-use.

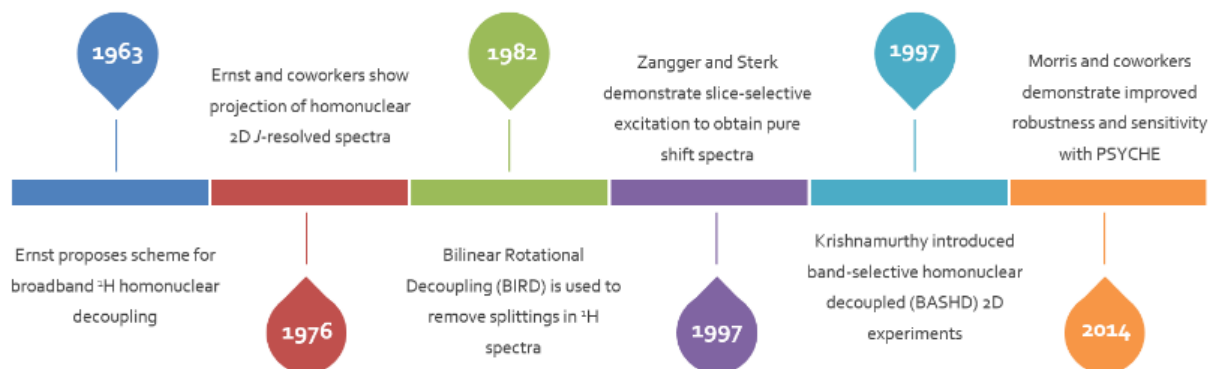


Figure 2. Brief timeline of key milestones in the development of pure shift NMR.

### Current Pure Shift Approaches

The popular pure shift experiments in use today are largely based on the important developments outlined above. At the heart of all current pure shift approaches is the concept of active and passive spins within the sample: active spins are those that contribute to the final signal, while passive spins do not.

In a pure shift experiment, the spins are manipulated by a specific pulse sequence element in such a way that the active spins are left unperturbed while the passive ones are inverted. The act of inverting the passive spins refocuses the J-evolution of the active spins, removing the splittings from the spectrum. The differing pulse sequence elements used to achieve this are often termed Active Spin Refocussing (ASR) elements[7].

#### Active Spin Refocussing (ASR) Elements

Fig. 3 shows ASR elements used in the most widely used pure shift experiments.

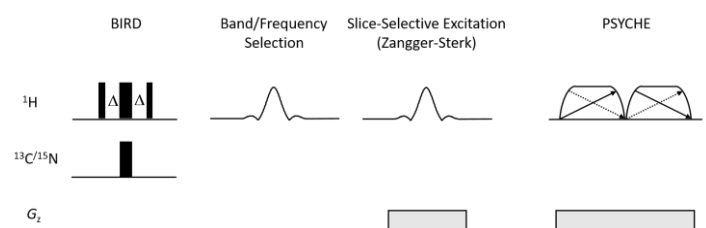


Figure 3. The main ASR elements used in pure shift experiments

Depending on the ASR element, the active and passive spins may be differentiated from each other based on their chemical shifts, their spatial locations within the sample (or in the case of the Zangger-Sterk element, both chemical shift and spatial location), or whether or not the spins are J-coupled to an NMR-active heteronucleus. As we will shortly see, different ASR elements are utilised in different experiments depending on the type of data being collected and the requirements for speed, sensitivity and spectral quality.

### Zangger-Sterk Experiment

The defining feature of the Zangger-Sterk experiment[5] is its use of slice-selective excitation, the principle of which is illustrated in Fig. 4. A frequency-selective pulse in the presence of a weak Z-axis field gradient is both chemical shift and spatially selective, that is to say, signals with different chemical shifts are excited in different horizontal slices of the sample.

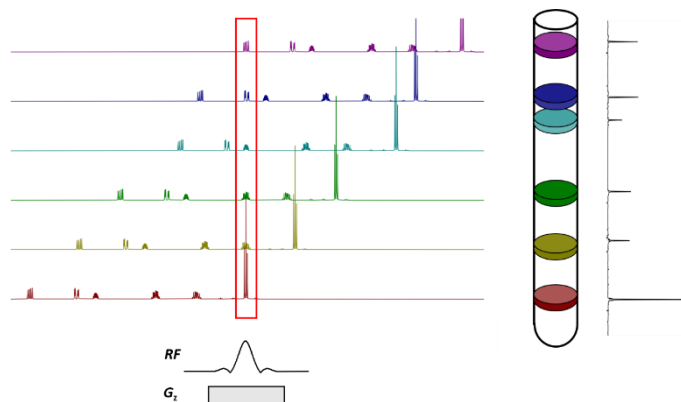


Figure 4. The principle of slice-selective excitation. The selective RF pulse excites magnetization in a narrow frequency band (red box), while the weak field gradient causes signals with different chemical shifts in different positions in the sample to “fall into” the frequency band of the selective pulse.

If the slice-selective RF pulse is a 180-degree pulse and is followed by a ‘hard’ (broadband) 180-degree pulse, the combined effect is to rotate the spins within each slice (the active spins) through 360 degrees, leaving them essentially unperturbed. In contrast, the passive spins originating from outside each slice experience only the hard 180-degree pulse and are thus inverted. This is the basis of the full Zangger-Sterk experiment.

### 'Chunked' Acquisition

The original Zangger-Sterk experiment uses an incremented  $t_1$  time period as in a 2D experiment. At the end of the  $t_1$  period, J-couplings are completely refocused while chemical shifts continue to evolve. The pure shift FID can then be constructed by taking the first point of the FID for each  $t_1$  period and concatenating them together. Unfortunately, as with the BIRD experiment, this point-by-point approach is very time consuming if a large number of points are needed to obtain a high-resolution spectrum.

However, Zangger and Sterk described an ingenious and in some ways surprising approach in which the pure shift FID could instead be constructed from 'chunks' of FID 'stitched' together rather than taking just the first data point of each FID. This chunked acquisition scheme works because proton-proton J-couplings are relatively small in magnitude, being only a few Hz, and so evolve much more slowly than the chemical shifts. If the chunks of data are kept short compared to the magnitude of the J-couplings, very little J-evolution occurs during each chunk and they can be stitched together with low-levels of artefacts in the resulting spectrum.

With chunked acquisition it is typical to acquire 32 or 64  $t_1$  increments using chunks of 10-20 ms in duration rather than the 1k or more increments that would be needed for the single-point method, thereby saving over an order of magnitude in time. The principle of chunked acquisition is illustrated in Fig. 5 below.

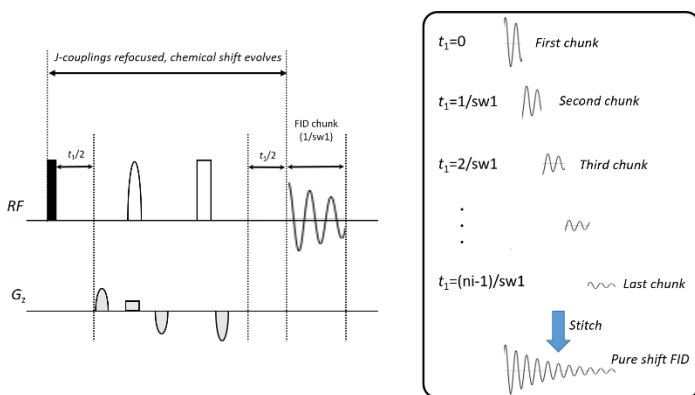


**Figure 5.** Principle of chunked acquisition using the Zangger-Sterk experiment.

Fig. 6 shows a typical result from the Zangger-Sterk experiment, collected on a sample of 2-ethyl-1-indanone. The pure shift spectrum was collected in 15 minutes using pseudo 2D acquisition, 4 scans per increment and 64 increments. Each multiplet in the conventional spectrum has been replaced in the pure shift experiment by a single peak. Note also that some small sidebands can be seen in the pure shift spectrum. These are the result of the chunked acquisition and are spaced by  $1/(\text{chunk width})$  from the main peak.

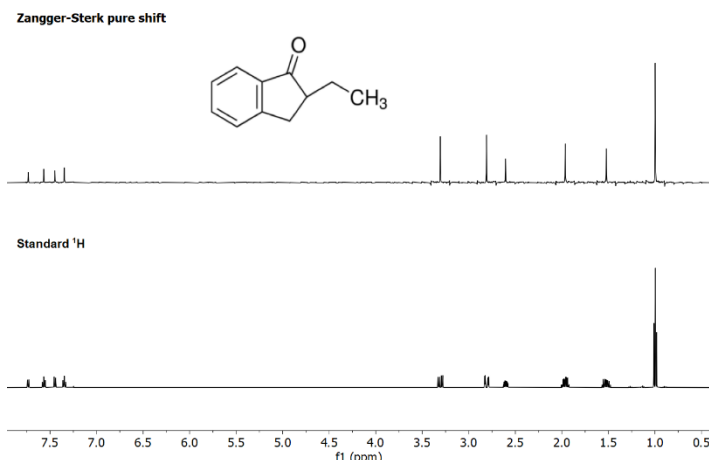


**Figure 6.** Comparison of standard  $^1\text{H}$  and Zangger-Sterk spectra collected on a sample of 2-ethyl-1-indanone. The data were collected on a JEOL ECZ-S 400 spectrometer equipped with a ROYAL HFX probe.

### Optimizing Slice-Selective Excitation

One of the drawbacks of Zangger-Sterk is the occasional need to adjust the slice selection depending on the spread of chemical shifts in the spectrum. If signals from J-coupled spins are close together, it may be necessary to reduce the bandwidth of the slice-selective pulse otherwise incomplete decoupling may result. Reducing the bandwidth of the pulse also means that the widths of the slices we detect magnetization from are narrower, which reduces sensitivity but yields higher purity spectra as illustrated in Fig. 7.

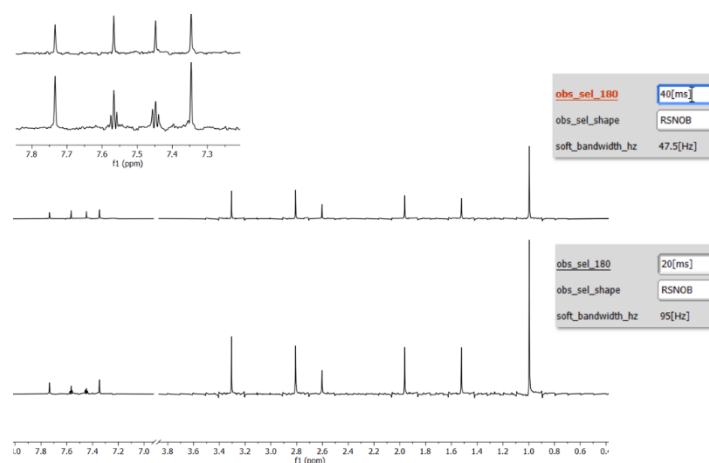


**Figure 7.** Effect of slice-selective pulse bandwidth on the pure shift spectrum. If the bandwidth is too wide, incomplete decoupling will result (bottom spectrum). Reducing the bandwidth of the pulse (increasing its duration) improves the decoupling, but with a loss in signal amplitudes (top spectrum).

### Real-time Zangger-Sterk Experiment

Another approach to collecting ZS spectra is to employ real-time acquisition[8] instead of the pseudo-2D method outlined above. Rather than acquiring the data in the form of a 2D experiment, it's possible to insert ZS elements directly into the FID acquisition period. This is done by alternating between acquiring a chunk of FID and executing a ZS element. The chunks of FID are then concatenated to give the pure shift FID (Fig. 8).

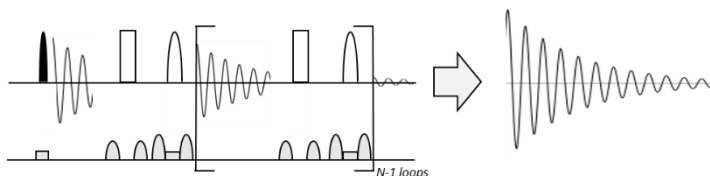


Figure 8. Real-time Zangger-Sterk experiment.

Real-time acquisition can greatly speed up the measurement of pure shift spectra, as Fig. 9 illustrates. The pseudo-2D experiment took 17 minutes to run, while the real-time acquisition was completed in under a minute.

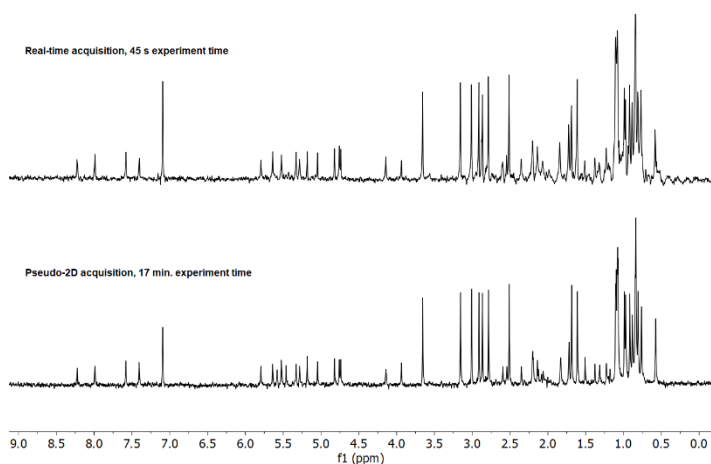


Figure 9. Comparison of Zangger-Sterk spectra of cyclosporine collected using pseudo 2D (bottom) and real-time (top) acquisition schemes. The data were collected on a standard JEOL ECZ-S 400 spectrometer equipped with a 5 mm ROYAL HFX probe.

Both spectra show similar signal-to-noise, so the sensitivity per unit time is clearly much higher in the real-time experiment and further improvements in signal-to-noise could be gained by accumulating more scans. The principal drawback of the real-time approach is generally lower spectral quality, with broader lines and more artefacts.

### HOBS experiment

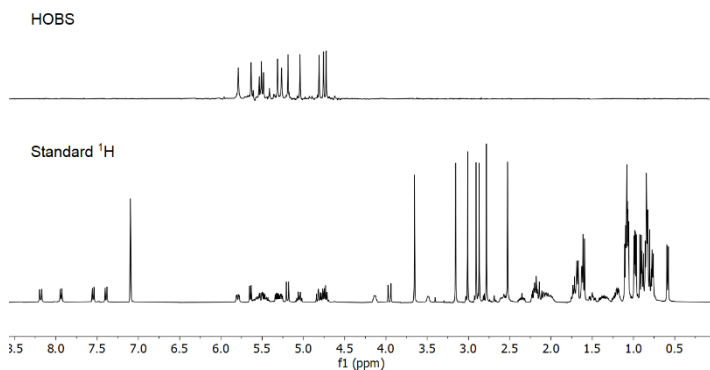
As we just saw, the Zangger-Sterk ASR element can be directly incorporated into the acquisition period to enable the acquisition of pure shift spectra in real-time. If the gradient is removed from the ASR element, the experiment becomes band-selective rather than slice-selective and only a region of the spectrum is excited: we now have the HOBS experiment[9] (Fig. 10).



Figure 10. The HOBS experiment in Delta 5.3.1.

Unlike the ZS experiment, HOBS does not yield a full pure shift spectrum; instead, signals that are excited by the band-selective pulse are decoupled from any signals that are outside the excited region (though mutually J-coupled spins that are in the excitation band are not decoupled from each other). This is an obvious disadvantage of HOBS compared to ZS, but the trade-off is much higher sensitivity: HOBS experiments provide full sensitivity compared to the standard proton experiment and, because multiplet structure is removed in the HOBS spectrum, the sensitivity is actually higher.

Fig. 11 shows a comparison of standard <sup>1</sup>H and HOBS spectra collected on a sample of cyclosporine. As can be seen, due to the collapse of many of the multiplets, the signal intensities in the HOBS spectrum are significantly higher. The average SNR for the HOBS experiment is over double that of the same region in the 1D proton. HOBS experiments can be particularly useful for analyzing spectra that contain one or more well-separated regions of signals where there is limited coupling between spins within the region of interest.



**Figure 11.** Comparison of HOBS and standard  $^1\text{H}$  spectra of a sample of cyclosporine. The data were collected on a standard JEOL ECZ-S 400 spectrometer equipped with a 5 mm ROYAL HFX probe. Both spectra are shown at the same absolute intensity.

### PSYCHE Experiment

There are two disadvantages of the Zangger-Sterk method. First, it usually suffers from poor sensitivity. Second, as we have seen, it can require careful adjustment of several of the parameters to get the best results, which makes it less than ideal as a routine experiment used by non-NMR experts. The PSYCHE experiment[6] (Fig. 12) largely overcomes those limitations.

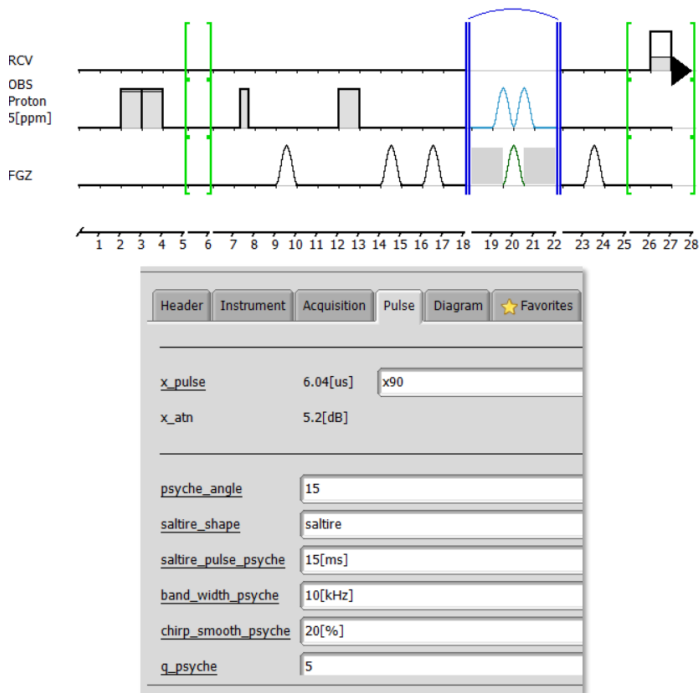


**Figure 12.** The PSYCHE experiment in Delta software.

In general, the only parameter in the PSYCHE experiment that is routinely adjusted is the flip angle of the chirp pulses (`psyche_angle` in Fig. 12). Depending on the flip angle used, there is a trade-off between the signal amplitudes in the PSYCHE spectrum and the spectral purity.

A larger flip angle gives more intense signals but with more artefacts, while a smaller flip angle reduces the signal intensities but gives cleaner spectra. For general use, a chirp flip angle of 10-20 degrees gives good results in the majority of cases. Fig. 13 shows an example PSYCHE spectrum of a sample of cyclosporine collected on a standard JEOL ECZ-R 500 spectrometer equipped with a 5 mm ROYAL HFX probe.

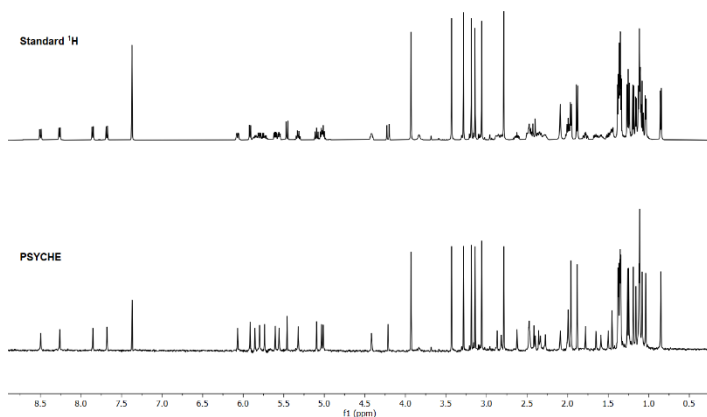


**Figure 13.** Comparison of standard  $^1\text{H}$  and PSYCHE spectra collected on a sample of cyclosporine.

The other significant advantage PSYCHE has over Zangger-Sterk is its generally higher sensitivity. Fig. 14 shows a comparison of ZS and PSYCHE spectra collected on a sample of cyclosporine. The ZS spectrum was collected in 15 minutes using 4 scans per increment and 64 increments - a 30 ms RSNOB refocusing pulse was used. The PSYCHE spectrum was recorded in 4 minutes with a single scan, 64 increments and a chirp flip angle of 20 degrees. The spectra are shown at the same absolute intensity. As can be clearly seen, the PSYCHE spectrum shows far higher signal intensities and higher signal-to-noise, despite having been collected in a quarter of the time.



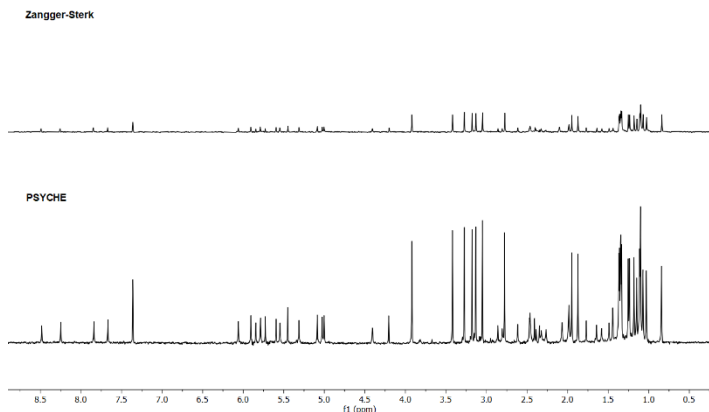


**Figure 14.** Comparison of Zangger-Sterk (top) and PSYCHE (bottom) spectra of cyclosporine. The data were collected on a standard JEOL ECZ-R 500 spectrometer equipped with a 5 mm ROYAL HFX probe. The Zangger-Sterk spectrum was collected using a 30 ms RSNOB pulse and the PSYCHE spectrum was collected using a 20-degree flip angle for the chirp pulses. Both are shown at the same absolute intensity to illustrate the significant sensitivity increase in the PSYCHE experiment.

PSYCHE is undoubtedly the most robust and easy-to-use general-purpose pure shift method to date, and is recommended as the first method to try when exploring pure shift methods.

#### Triple Spin Echo (TSE) PSYCHE

The standard PSYCHE experiment is a robust experiment that produces fairly clean pure shift spectra with decent sensitivity (for a pure shift experiment) on a wide range of samples. However, while it is quite tolerant of strong coupling (i.e. where the chemical shift difference between J-coupled spins is comparable or not much larger than the magnitude of the couplings), it is not completely immune to its effects and strong coupling artefacts can often persist. A modification to the standard PSYCHE experiment to incorporate two additional 180-degree chirp pulses in the presence of weak gradients attenuates these strong coupling artefacts, often yielding a much cleaner spectrum[10].

It should be noted that this is usually at the expense of a loss of signal intensity in the pure shift spectrum. However, the signal-to-artefact ratio, which is generally more important than signal-to-thermal noise, is often higher in the TSE-PSYCHE spectrum. Fig. 15 shows an example from a sample of 2-ethyl-1-indanone. As can be seen, there is appreciable strong coupling in the aromatic region of the spectrum, giving rise to strong coupling artefacts in the PSYCHE spectrum (denoted by red asterisks). These strong coupling artefacts are completely attenuated in the TSE-PSYCHE spectrum.

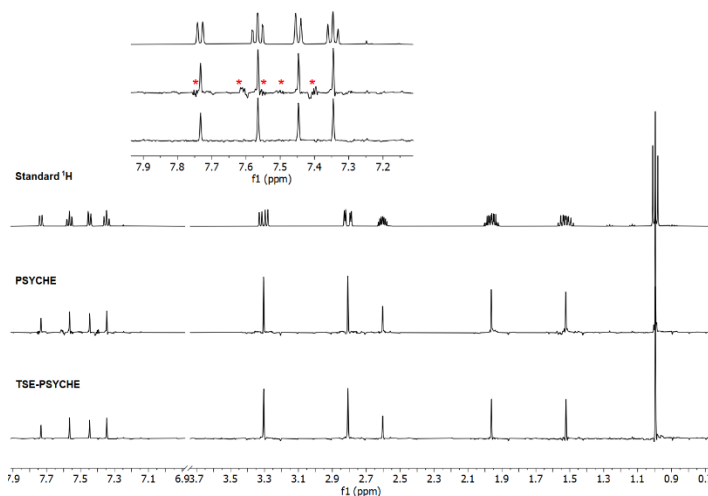


**Figure 15.** Comparison of standard  $^1\text{H}$ , PSYCHE and TSE-PSYCHE spectra. Strong coupling artefacts are visible in the aromatic region of the PSYCHE spectrum (indicated with asterisks) but are absent in the TSE-PSYCHE spectrum.

#### Incorporating PSYCHE into 2D experiments

The basic PSYCHE ASR element can be readily incorporated into the  $t_1$  evolution period of a number of 2D experiments to remove homonuclear splittings from the  $F_1$  dimension of the spectrum. For example, Fig. 16 shows a comparison of a standard 2D TOCSY spectrum (top-left) with an  $F_1$  PSYCHE-TOCSY spectrum (top-right), collected on a JEOL ECZ-S 400 spectrometer equipped with a ROYAL HFX probe. As can be seen, the resolution in the  $F_1$  dimension of the  $F_1$  PSYCHE-TOCSY spectrum is much higher due to the removal of the homonuclear splittings. The resolution can be further improved by applying covariance processing to the spectrum to yield a double pure shift TOCSY spectrum (bottom right).

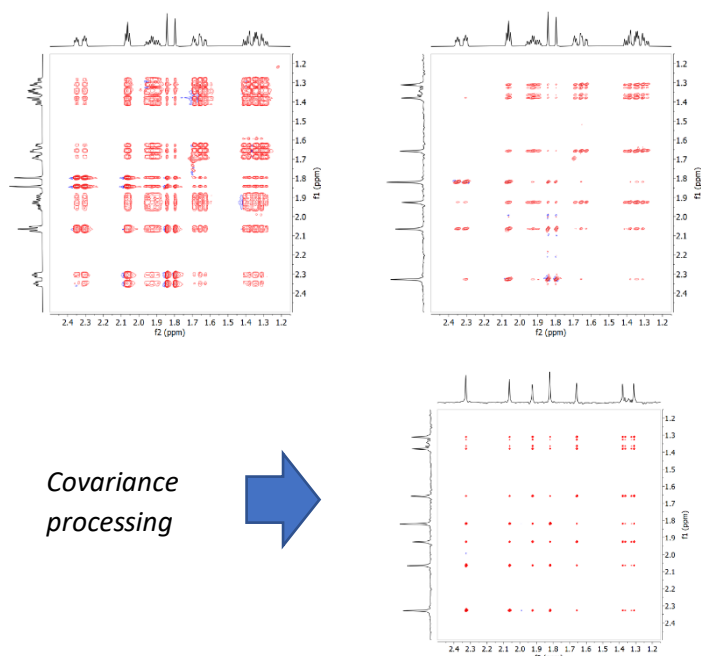


**Figure 16.** Comparison of standard 400 MHz TOCSY spectrum of camphor (top left) with  $F_1$  PSYCHE TOCSY spectrum (top right). The  $F_1$  PSYCHE TOCSY spectrum can be covariance processed to give a double pure shift spectrum (bottom right).

### Pure shift HSQC

The BIRD pulse sequence element (see Fig. 2) enables the selective inversion of protons bound to an NMR-inactive heteronucleus (e.g.  $^{12}\text{C}$ ) while leaving protons bound to its NMR-active counterpart ( $^{13}\text{C}$ ) unperturbed. This behaviour of BIRD has led to its use in heteronuclear 2D experiments such as  $^1\text{H}$ - $^{13}\text{C}$  HSQC, most commonly to help suppress the large, unwanted responses from protons attached to  $^{12}\text{C}$  atoms (“BIRD nulling”). However, BIRD also can be put to great use as an active spin refocussing element to achieve broadband homonuclear decoupling in HSQC[12]. Just as with the real-time Zangger-Sterk experiment, where the acquisition of the FID is broken up into chunks and a ZS ASR element inserted between each chunk, in pure shift HSQC the BIRD ASR element is inserted between chunks of FID recorded during the  $t_2$  acquisition period.

The action of the BIRD element between each chunk is to invert the protons bound to  $^{12}\text{C}$ , which do not contribute to the final signal, while leaving the protons of interest, bound to  $^{13}\text{C}$ , unperturbed. The continual inversion of the  $^{12}\text{C}$ -bound protons during the  $t_2$  acquisition period therefore decouples those passive protons from the active (observed) ones and gives an HSQC spectrum free of homonuclear splittings, with the exception of those responses from non-equivalent methylene protons. In those cases, it is not possible to decouple those protons from one another using BIRD because the two protons are bound to the same carbon atom, whether it be a  $^{12}\text{C}$  or  $^{13}\text{C}$ . Consequently, the signals from non-equivalent methylenes appear as doublets in the pure shift HSQC spectrum.

Unlike nearly all other pure shift methods, pure shift HSQC does not pay a sensitivity penalty compared to the conventional experiment, because the magnetization detected in HSQC has already been “filtered” through the NMR-active heteronucleus. In fact, owing to the fact that  $F_2$  multiplets in the conventional spectrum are replaced by more intense singlets in the pure shift spectrum, the sensitivity is often higher in the pure shift spectrum.

Fig. 17 shows two regions of the HSQC and pure shift HSQC spectra of a sample of glucose, and illustrates the main features of this experiment described above.

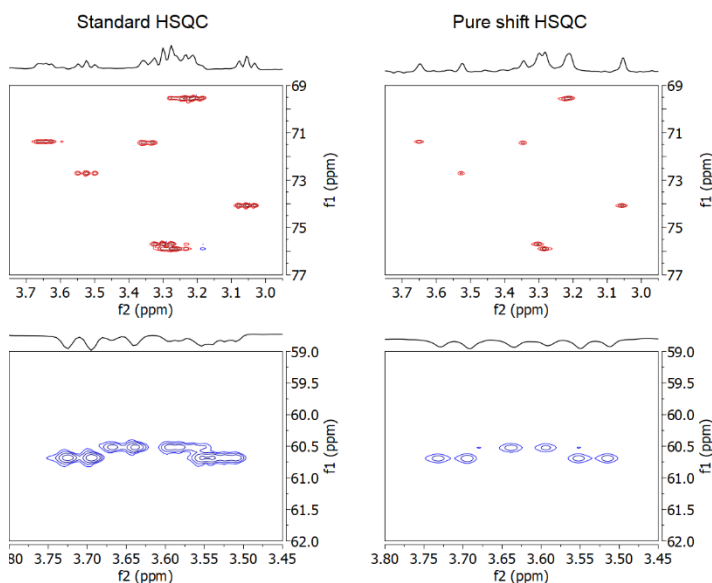


**Figure 17.** A comparison of standard (left) and pure shift (right) HSQC spectra of sample of glucose (two expanded regions shown for clarity). The data were collected on a standard JEOL ECZ-S 400 spectrometer equipped with a 5 mm ROYAL HFX probe. The pure shift HSQC exhibits significantly higher resolution in the proton ( $F_2$ ) dimension. Signals from non-equivalent methylene protons (bottom spectra) are shown as doublets in the pure shift spectrum.

### Conclusions

As has been outlined in this paper, pure shift NMR has developed considerably since the initial concept was proposed several decades ago. Newer experiments like PSYCHE are robust and easy enough for routine use and provide improved sensitivity. JEOL Delta software provides a comprehensive suite of 1D and 2D pure shift experiments that can be set up and run easily and provide high-quality pure shift spectra.

## References

1. R.R. Ernst, H. Primas, *Helv. Phys. Acta* **1963**, 36, 583-600.
2. W.P. Aue, J. Karhan, R.R. Ernst, *J. Chem. Phys.* **1976**, 64, 4226-4227.
3. J. P. Garbow, D. P. Weitekamp, *A. Pines. Chem. Phys. Lett.* **1982**, 93, 504-509.
4. K. Zangger, H. Sterk. *J. Magn. Reson.* **1997**, 124, 486-489.
5. V. V. Krishnamurthy. *Magn. Reson. Chem.* **1997**, 35, 9-12.
6. M. Foroozandeh, R.W. Adams, N.J. Meharry, D. Jeannerat, M. Nilsson, G.A. Morris, *Angew. Chem. Int. Ed.* **2014**, 53, 6990-6992.
7. L. Castañar Acedo, Workshop on Pure Shift NMR, Sept. 12th, 2017.
8. N.H. Meyer, K. Zangger, *ChemPhysChem* **2013** 15, 49-55.
9. L. Castañar, P. Nolis, A. Virgili, T. Parella. *Chem. Eur. J.* **2013**, 19, 17283-17286.
10. M. Foroozandeh, R. W. Adams, P. Kiraly, M. Nilsson, G. A. Morris, *Chem. Commun.*, **2015**, 51, 15410–15413.
11. M. Foroozandeh, R.W. Adams, M. Nilsson, G.A. Morris, J. *Am. Chem. Soc.* **2014**, 136 11867-11869.
12. L. Paudel, R. W. Adams, P. Kiraly, J. A. Aguilar, M. Foroozandeh, M. J. Cliff, M. Nilsson, P. Sandor, J. P. Waltho, G. A. Morris, *Angew. Chem. Int. Ed.* **2013**, 52, 11616 -11619.